

# Impulsive processes in the magnetotail during substorm expansion

V.A. Sergeev<sup>1</sup>, T. Bösinger<sup>2</sup> and A.T.Y. Lui<sup>3</sup>

<sup>1</sup> Institute of Physics, University of Leningrad, Leningrad 198904, USSR

<sup>2</sup> Department of Physics, University of Oulu, SF-90570 Oulu 57, Finland

<sup>3</sup> Applied Physics Laboratory, The Johns Hopkins University, Laurel, MD 20707, USA

**Abstract.** Anisotropy and intensity variations of high-energy particles and magnetic variations detected by IMP-J at 37  $R_e$  in the central part of the magnetotail within 2  $R_e$  of the neutral sheet were studied during a few consecutive substorms on March 3, 1976, and related to a large body of ground observations. A close correlation is usually found between bursts observed in Pi pulsations on the ground (having a duration of  $\sim 1$  min and usually being repeated in 1–3 min) and high-energy particle bursts observed in the far tail. The magnetic field response is examined relative to the onsets of high-energy particle bursts. A three-dimensional current system RIPD (Reconnection Induced Propagating Disturbance) is constructed which can, in principle, produce the magnetic field variations observed in the boundary part of the plasma sheet (PS). Previously reported properties of high-energy particle bursts (inverse energy dispersion, preferential acceleration of alpha particles, dawn-dusk asymmetry in the acceleration of electrons and protons and transient PS expansions) are found to be typical of these impulsive processes. Together with earlier results, these observations show that the expansion process (identified here as a transient reconnection or explosive tearing mode) clearly operates in an impulsive fashion. The superposition of impulse-induced propagating disturbances necessarily results in complex, variable patterns of magnetic field and thermal plasma behaviour, such as are frequently found in the PS during substorms.

**Key words:** Substorm expansion – Magnetotail-ground correlation – Plasma sheet boundary – High-energy particle bursts – Propagating magnetic field disturbance

## Introduction

The substorm expansion process includes a change in the gross structure of the magnetotail magnetic field and plasma configuration accompanied by strongly enhanced energy dissipation in the magnetosphere-ionosphere system. Detailed synthesis of plasma sheet (PS) phenomena observed to date (such as plasma flow and energization, magnetic and electric field variations, etc.) is still a subject giving rise to many controversies, and consequently there are not yet any well-developed theoretical models available.

The authors of numerous papers on substorm morphology in the PS nevertheless seem to agree on certain major findings. These include:

a) A source at 10–15  $R_e$  distance in the night-time magnetotail is turned on and later displaced tailward in some way (stepwise and/or continuously) during the substorm expansion phase (Pytte et al., 1976; Nishida and Fujii, 1976; Hones et al., 1973).

b) Earthward of this source strong plasma flows tend to exist, mainly in an earthward direction, and the magnetic field relaxes somewhat towards a more dipole-like configuration in conjunction with the PS expansion (Pytte et al., 1976; Lui et al., 1976; Hones, 1979 and others).

c) Tailward of the source the direction of strong plasma flows and the polarity of the  $B_z$  component of the magnetic field are variable and complex, but tailward plasma flows and southward turnings of  $B_z$  are quite common (Lui et al., 1977; Hones and Schindler, 1979; Nishida et al. 1981; Caan et al., 1979 and others).

d) A strongly enhanced, newly accelerated, high-energy (HE) particle population up to MeV energies is found, which propagates from the source both tailwards and earthwards (Krimigis and Sarris, 1979; Baker et al., 1982).

The characteristics mentioned above depict only a type of average behaviour, and the numerous discrepancies in the details of PS observations indicate a complex space-time evolution of the substorm process in the tail (Coroniti et al., 1980). This seems to operate in a sporadic manner (time scales from 10 s to several minutes have been distinguished) in localized parts of the PS (Pytte et al., 1976, 1978; Sergeev, 1977, 1981; Krimigis and Sarris, 1979; Belian et al. 1984), and there are even indications of the simultaneous presence of several sources (Sarris et al., 1976b).

The interpretation of PS observations is particularly problematical because temporal and spatial variations are difficult to separate on the basis of single-satellite measurements. The situation is further complicated because of the different propagation speeds involved (e.g. MHD, plasma drift and HE particle speeds). Williams (1981) has demonstrated that, due to dispersion, a wealth of energy and pitch-angle distributions of energetic ions exists (after the step-like process of ion acceleration) even in the relatively simple case of non-interacting particles. Possibly the most serious difficulty in the interpretation of PS observations arises when large-scale effects of the source are masked by disturbances of local origin (e.g. strong turbulence, as apparently identified by Coroniti et al., 1980). These difficulties are

well known, but to our knowledge they have not yet been explicitly taken into account.

It seems possible, however, to isolate large-scale effects from small-scale ones, namely when the source acts in an impulsive fashion, provided we are looking at the phenomena on a time-scale which is small in comparison with the duration of the impulse. There are indeed facts which speak in favour of an impulsively operating source. First there are the observations of large impulsive electric fields (Aggson et al., 1977; Pedersen et al., 1978; Cattell et al., 1982), and then there are reports on multiple short HE particle bursts and injections (Krimigis and Sarris, 1979; Lui and Meng, 1979; Kirsch et al., 1981; Baker et al., 1982; Belian et al., 1984). Impulsive or step-like behaviour in the sub-storm expansion process has been inferred from ground-based observations (here the temporal and spatial effects can be clearly separated). In this way Sergeev et al. (1978) were able to elucidate the fine structure of auroral expansion. Practically all studies based on high time resolution ground observations, including auroras, currents, HE electron precipitations and ULF-waves, have confirmed that the expansion process operates in an impulsive manner characterized by a time-constant typically of 1–3 min (e.g. Sergeev and Yahnin, 1979; Bösinger et al., 1981; Yahnin et al., 1983). This holds for expansions of different strength and different spatial extent (Yahnin et al., 1983). Impulsive HE particle injections with similar temporal characteristics were found to be common at geosynchronous distance (Belian et al., 1984).

As will be seen below, HE particle bursts often show a remarkable correspondence with impulsive modulation of the expansion process as observed on the ground. This is true even in cases of very weak, small-scale expansions (Yahnin et al., 1984).

The aim of this paper is two-fold: firstly, to provide a detailed ground – satellite comparison to show once again the impulsive behaviour of the expansion process and, secondly, to monitor changes in the PS magnetic field and HE particles after the switching on of the source in order to construct a phenomenological scheme of manifestations of the expansion process in the far PS.

Since the behaviour of HE particles in the 0.3–2.0 MeV energy range (i.e. energies 2–3 orders of magnitude larger than the thermal energy of PS particles) is considered here to be of crucial importance, we recall below some of their properties as given in the literature (Buck et al., 1973; Krimigis and Sarris, 1979; Williams, 1981; Andrews et al., 1981; Belian et al., 1981 and others):

1. At IMP-J distance ( $37 R_e$  in the magnetotail, in our case) the gyroradius of the HE protons ( $1 R_e$ ) is comparable to both the PS thickness and – in our case – the distance of the satellite from the PS centre. This allows the HE protons to be seen almost all the time during expansion, and also allows the spatial and temporal effects to be distinguished and the configurational changes of the PS to be investigated to some extent (N–S displacements of its boundary).

2. Since the protons in the bursts are highly anisotropic and are collimated mainly along the magnetic field lines, we have information on the source location (tailward or earthward with respect to the satellite). Due to the high speeds of the HE particles (tens of  $R_e/s$  for electrons), their arrival time forms a reference time for the study of the concurrent thermal plasma and magnetic field behaviour.

## Instruments, data and observations

### *General correspondence between HE particle bursts and ground activity, characteristics of the period studied*

The most important PS parameters studied here were obtained from the GSFC magnetometer and two energetic-particle detectors on board the IMP-J satellite. We use the 15.36-s averages of the magnetic field vector expressed either in the GSE or GSM coordinate system, and the standard deviation ( $\sigma$ ) of individual 1.28-s measurements. This quantity characterizes the field variability or magnetic fluctuations below 1 Hz. The particle detectors (the APL/JHU experiment CPME, for details see Sarris et al., 1976a) provide information on the HE proton and electron fluxes in a few energy channels above 0.3 MeV. Alpha-particle fluxes are measured above 2 MeV. A complete cycle comprises measurements made during a 5.12-s interval repeated every 10.24 s and provides information on the particle fluxes in eight angular sectors of the ecliptic plane. We also use data on 50–200-keV protons from the EPD experiment (for details, see Roelof et al., 1976), which yields better angular resolution (data from 16 sectors of the ecliptic plane) but only every 20.48 s.

During the period of interest the IMP-J satellite made measurements in the central part of the magnetotail, moving from dusk towards midnight. Its GSM coordinates in  $R_e$  early and late on March 3, 1976 read  $-34.8, 16.3, 0.1$  and  $-36.7, 0.5, 3.1$ , respectively. Because of fortunate details of both the satellite orbital motion and the diurnal movement of the neutral sheet, the satellite stayed within  $2-3 R_e$  of the PS centre throughout the day (see the bottom curve in Fig. 1). This extremely rare and fortunate circumstance permits us to consider the association between HE particle bursts and different ground-based observations during various kinds of magnetospheric activity. The second fortunate circumstance is the large number of available ground-based observations obtained from the world-wide networks of magnetometers, all-sky cameras, photometers, riometers, induction magnetometers, etc.. The data were collected and analysed in an informal workshop devoted to the global and local relationship between different ground phenomena during substorms. Much of the data collected has been published (Sergeev et al., 1981; Mishin et al., 1982), and the results of the analysis are collected in a special issue (Pudovkin and Sergeev, 1984). We will refer extensively to these publications below. Information on the ground-based instrumentation can be found in Sergeev (1981).

As can be seen from the upper panel of Fig. 1, the day concerned is characterized by various types of magnetic activity. It contains an 8-h period of intense and prolonged activity, well-pronounced substorms – both isolated and superimposed – and also a 3-h long quiet period between 13 and 16 UT. It also shows significant HE particle activity, the intensity of which generally reflects the behaviour of the AE index. These time intervals, based on 5.5-min averages, are marked by black spaces in Fig. 1, sequences which contain strong fluxes of 0.5-MeV electrons (HEE) and 3-MeV protons (HEP). Threshold fluxes of  $1 \cdot (\text{cm}^2 \cdot \text{s} \cdot \text{ster})^{-1}$  for HEE and  $3 \cdot 10^3 (\text{cm}^2 \cdot \text{s} \cdot \text{ster} \cdot \text{MeV}/\text{nucl})^{-1}$  for HEP are chosen, which are a factor of three higher than the maximum values during the quiet interval of 15–16 UT, when the satellite stayed within the PS. HE particles were pre-

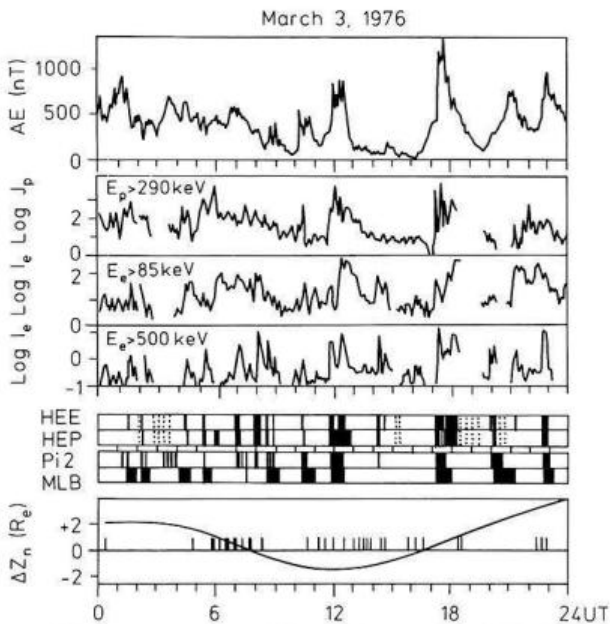


**Fig. 1.** Magnetic and particle activity on March 3, 1976. From top to bottom: AE(7) index; 5.5-min averages of differential proton ( $J_p$ ) and integral electron ( $I_e$ ) flux intensities measured by the EPD and CPME experiment on board the IMP-J satellite; intervals (indicated by black space) of most intense electron (HEE) and proton (HEP) particle bursts (for details, see text); intervals (black space) of Pi-2 activity (Pi2) and magnetic bays (MLB) as observed at nightside mid-latitude observatories; the distance ( $\Delta Z_n$ ) of IMP-J from the calculated position of the neutral sheet (the vertical bars indicate times of neutral sheet crossings, i.e. changing polarity of the  $B_x$  component), is from IMS/SSC report N 5, 1975

ferred as tracers, since these particles exit faster from the acceleration region (due to their higher drift speeds). Consequently, the time intervals of peak HE particle flux indicate the time intervals of particle acceleration more accurately and reliably. Note also that the gyroradius of a 3-MeV proton in the lobe field (2–3  $R_e$ ) is larger than the distance of the satellite from the neutral sheet during the whole period of observation. The dotted lines indicate gaps in the IMP-J data. One can see that the time intervals of the strong fluxes in the highest energy channels are, in general, the same for particles of both types.

Let us first compare the appearance of these HE particle bursts with the ground signatures of substorm expansion. The two lower panels of Fig. 1 (marked Pi2 and MLB) indicate the time intervals during which expansion-related Pi2 pulsations and magnetic bays are seen at mid-latitudes (standard, rapid-run and induction magnetometer data from the world-wide networks are used). As already known for HE particle bursts (Murayama, 1970) and for other expansion-related signatures of the magnetotail (Pytte et al., 1976, 1978), the bursts tend to appear in close association with Pi2s and mid-latitude bays whenever the activity is continuously high (as before 08 UT) or low. One remarkable example of this association is the very strong HE particle burst detected around 14:15 UT during conditions of magnetic calm (AE  $\sim$  100 nT). The few exceptions from this close temporal correlation may be consequences of the known screening effect (Pi2 intensity is strongly damped at mid-latitudes when the expansion proceeds beyond 70° corrected geomagnetic latitude (CG Lat); see examples in

Wolcott et al., 1976; Pytte et al., 1978 and also Sergeev, 1981).

The typical pattern of the proton flux and its anisotropy during substorm expansion is best depicted by an isointensity-contourline presentation, as used earlier by Roelof et al. (1976). Figure 2 contains such presentations for the two clearest and most intense substorms observed on March 3, 1976, (onsets at 11.51 and at 17.16 UT, cf. Sergeev, 1981). The gross features of these substorm expansions are similar in terms of the HE particle characteristics, although IMP-J spent most of the time within the PS during the first event and outside it during the second, as evidenced by the magnetic field and thermal plasma data (E.W. Hones, personal communication). These common features include strong tailward anisotropy during the first stage (the first 20 min in these cases), and strong earthward anisotropy during the second stage up to the final PS expansion. The spot-like appearance (intense, collimated particle bursts) during the first 40 min in each case in Fig. 2 deserves special attention, since it reflects a burst-like particle behaviour (more pronounced in the higher energy proton channels). The HE particle bursts during the interval 17:32–17:34 UT were examined in detail by Lui and Krimigis (1983) and were found to be hot beams with low densities and high drift speeds. With reference to Fig. 2 and similar presentations by Roelof et al. (1976), Carbary and Krimigis (1979) and similar findings by Lui and Meng (1979), we can say that series of repetitive HE particle bursts with repetition periods of 1–3 min form a typical feature of the expansion phase.

In Fig. 2 another interesting feature can be noted. There are sporadically occurring signatures of counterstreaming HE proton flows (flux contours are centred at both 180° and 360°). These signatures are particularly clear from 17.29 to 17.32 UT and 17.42 to 17.49 UT. The observation of counterstreaming HE protons is not unusual (see e.g. Williams, 1981). It should be noted, however, that the parent beam (tailward between 17.10 and 17.35 and earthward between 17.42 and 17.50 UT) exceeds the oppositely directed flux by more than one order of magnitude. This kind of counterstreaming may be understood in terms of return fluxes caused by magnetic mirroring or magnetic loops.

In all the substorm cases of March 3, 1976 the series of particle bursts appear synchronously with enhanced Pi activity (Pi2 at mid and auroral latitudes, Pi1B in the nightside auroral zone). Often, however, it is hard to recognize unambiguously the overlapping effects of individual bursts and to identify the intensifications observed on the ground with these individual HE particle bursts. For the purpose of ground-satellite comparison we will therefore present a case below in which the HE particle bursts are well separated in time.

#### *An example of detailed PS – ground correlation*

As evidenced by ground-based observations, the substorm which initiated at 19:59:00 UT developed mostly within the Scandinavian sector. Because of this temporal variation and the relationships between phenomena such as auroral structures, brightness and heights, cosmic noise absorption, equivalent currents and Pi2/Pi1B type magnetic pulsations could be studied in great detail and with high temporal and spatial resolution. Readers are referred to the companion paper by Sergeev et al. (1986, referred to as paper II

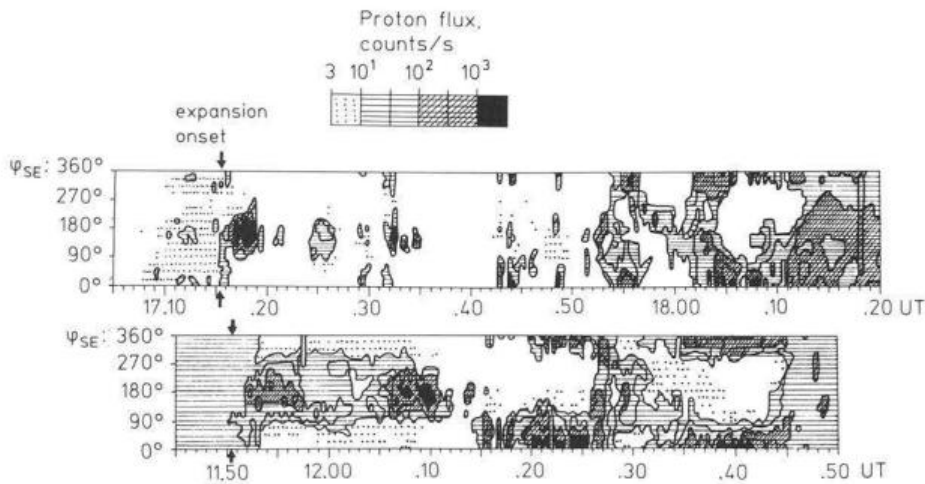


**Fig. 2.** Azimuthal proton fluxes ( $E_p = 50\text{--}200$  keV) in isocontourline presentation as measured by the EPD detector of IMP-J in the ecliptic plane during the two most intense substorms of March 3, 1976 ( $\psi_{SE} = 0^\circ, 90^\circ, 180^\circ$  correspond to earthward, dawn-to-dusk and tailward directions, respectively)

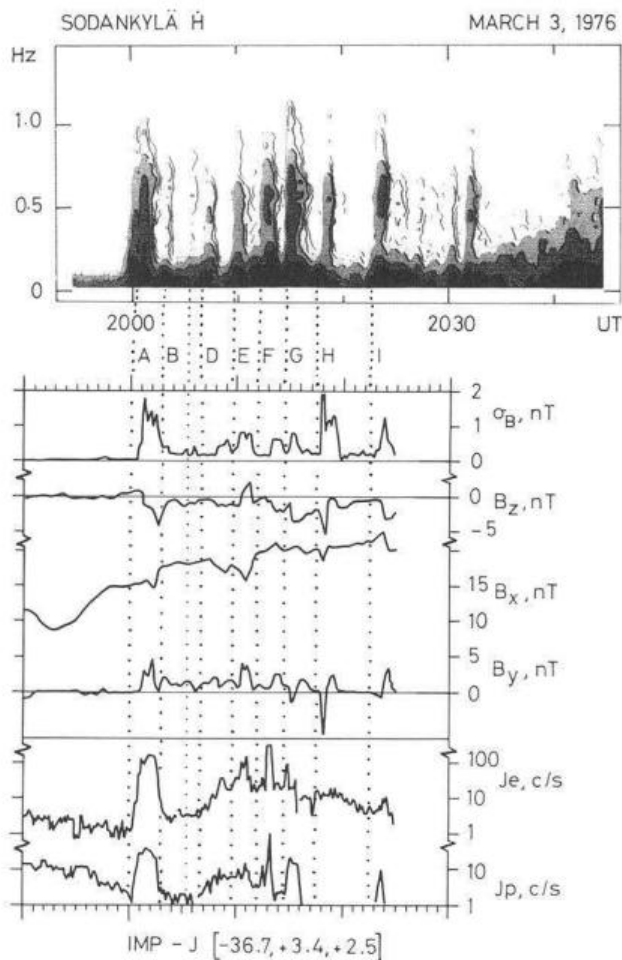


**Fig. 3.** Sonogram showing successive Pi1 bursts as recorded at Sodankylä ( $\phi = 63.8^\circ$ , MLT = 22.5 h) during the expansion phase of the substorm commencing at 19:59 UT on March 3, 1976 (top). Summary of IMP-J magnetic field and particle data ( $E = 0.3\text{--}0.5$  MeV) as measured in the boundary part of the plasma sheet up to the data gap of 20:25 UT (bottom). The magnetic field components are displayed in the GSM coordinate system. The IMP-J projection into the ionosphere lies at 23.1 MLT meridian. Dotted lines indicate times of onset of Pi1 burst. To convert count rates into fluxes, use a geometry factor of  $1.51 \text{ cm}^2 \text{ ster}$

in the following). We reproduce here, in the upper part of Fig. 3, a sonogram of the induction magnetometer record from Sodankylä, which gives the onsets and relative intensities of a dozen well-defined impulsive activations which occurred during the first half-hour of the substorm expansion.

This time the IMP-J was gradually leaving the thinning PS, as evidenced by a gradually increasing  $B_x$  component (Fig. 3) and a decreasing energy density in the thermal plasma (E.W. Hones, personal communication). Shortly after the first ground signatures of the expansion onset (19:59–20:00 UT, see paper II) the substorm manifests itself at a distance of  $37 R_e$  in the central magnetotail by a significant increase in HE particle fluxes and by the onset of magnetic field fluctuations  $\sigma$  and variations in all three components (Fig. 3). The onsets of all the impulsive activations, as detected on the ground, are given in Fig. 3 by dotted lines labelled A, B, D, E, F, G, H and I. The activation C (between B and D) is very weak but nevertheless included (dotted line, but not labelled) here because it is dealt with in paper II. Almost simultaneous impulsive changes in the magnetic field and the HE particle fluxes at IMP-J can be recognized. There is not only a temporal correspondence between the ground and IMP-J observations, but there is also a similar intensity response of the Pi1Bs to spikes in the particle fluxes. The most prominent HE particle bursts are associated with the activations A, E, F and H, which appear to be the strongest ones in terms of their other ground signatures as well (see paper II).

In order to obtain information on the time delays between phenomena observed on the ground and at the boundary of the PS, we restrict our analysis to the most intensive particle bursts (in which the concurrent magnetic field variations can be expected to be well above the background noise). The broken lines in Fig. 4 denote onsets of HE bursts, which are distinct in the protons and the electrons. Both the superimposed (F, G) and isolated impulses (A, I), are followed by a distinct rise in  $\sigma$  and an impulsive negative excursion of  $B_z$  (dotted lines). The time delay ranges from 0 s (I) to 50 s ( $A_2$ ). Similarly, the appearance of the HE bursts seems to be delayed relative to the onsets of Pi bursts observed on the ground. Both the delays and their tendency to decrease in the course of the expansion can be explained by the relative position of the satellite with respect to the source region. As in the first stage of the cases shown in Fig. 2, the proton flow in the ecliptic



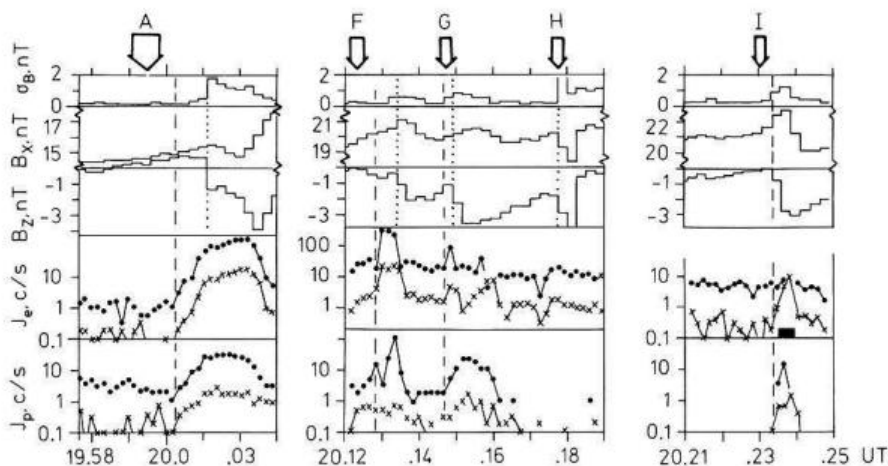


**Fig. 4.** High-resolution data of the magnetic field (15.36 s) and spin-averaged (10.24 s) particle count rates for the periods of intense particle bursts in Fig. 3. Onsets of the particle bursts and impulsive negative  $B_z$  excursions are indicated by broken and dotted lines, respectively. The arrows at the top of the figure mark the Pi1 burst onset (cf. Fig. 3)

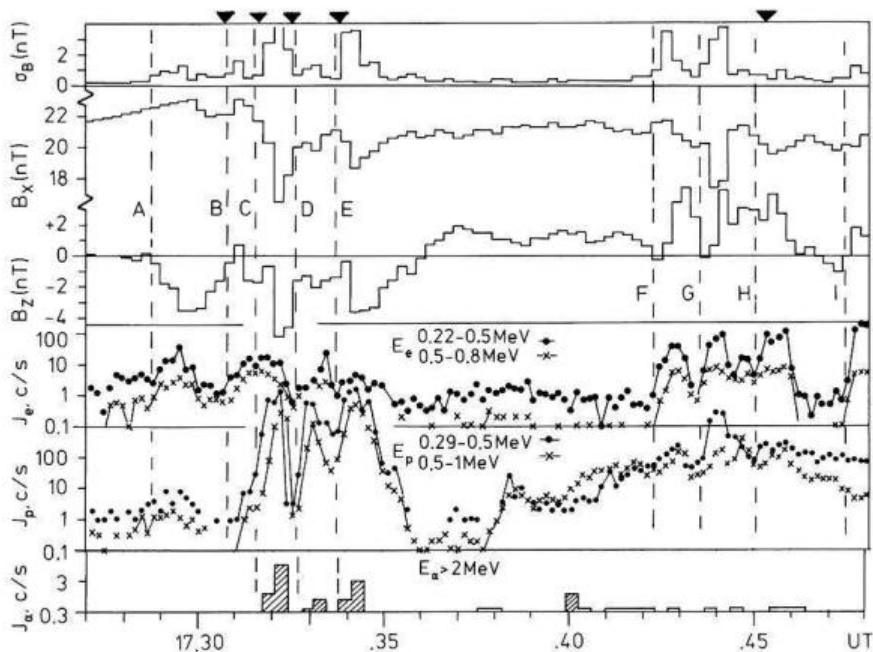


**Fig. 5.** Data as in Fig. 4, but for the most intense substorm observed on March 3, 1976. The count rates of alpha particles are added in the bottom panel. Distinct impulsive changes in Pi2 signals are marked by triangles at the top of the figure. Lines with dots or crosses denote the 0.29–0.50 MeV and 0.5–1.0 MeV energy channels, respectively. Note that the proton fluxes are highly anisotropic during this interval and are directed tailwards before 17:36 UT and earthwards after 17:42 UT (cf. Fig. 2)

plane was found to be highly anisotropic and oriented in a tailward direction (almost) along the magnetic field lines. From this we can conclude that the source during this period is located somewhere between the Earth (behind  $10 R_e$ , to be exact) and the satellite ( $37 R_e$ ). From the auroral-zone data we know that the auroral expansion started at  $66^\circ$  CG Lat and expanded polewards in a stepwise fashion, reaching  $71^\circ$  CG Lat at 20:23 UT (paper II). Correspondingly, we can assume that in the course of the successive activations the source region is displaced tailward (towards the satellite), which gives a natural explanation for the decreasing time delay. If so, we can further argue that the observed negative excursion of  $B_z$ , which is largest in the first activation, is caused by some current system which propagates in the PS with a speed lower than that of the HE particles.

Returning to the magnetic variations in the PS shown in Fig. 3, we can note the following. First of all, there is no simple correlation between the magnetic field variation amplitude and the intensities of the HE and/or Pi1 bursts. The event G, for example, shows a very intense magnetic

field variation (possibly of local origin) with no significant HE particle response. Then, by comparing the variations in  $B_z$  and  $B_y$  relative to their levels both before the onset of the substorm and a few minutes prior to the isolated activation I, we can conclude that their response to the impulsive activations constitutes mainly a negative excursion for  $B_z$  and a positive one for  $B_y$ . Exceptions, however, are evident, particularly the positive  $B_z$  variation after activation E. Variations in the largest component, namely  $B_x$ , are less distinct, probably because of the continuous growth of the tail current at IMP-J position. For the most intense HE particle bursts seen in Fig. 4, a rise in  $B_x$  in the first 30 s (after the onset of the burst) and then a drop below the previous level seems to be typical.

Intense HE proton bursts in both channels ( $>0.3$  and  $>0.5$  MeV) are observed only during three activations (A, G, I). Indications of inverse energy dispersion (0.3-MeV protons arrive and/or reach the maximum flux first) show impulse G and impulse I in Fig. 4. A brief appearance of HE alpha particles above 2 MeV is detected at the maximum phase of activation A (20:00:53 UT).

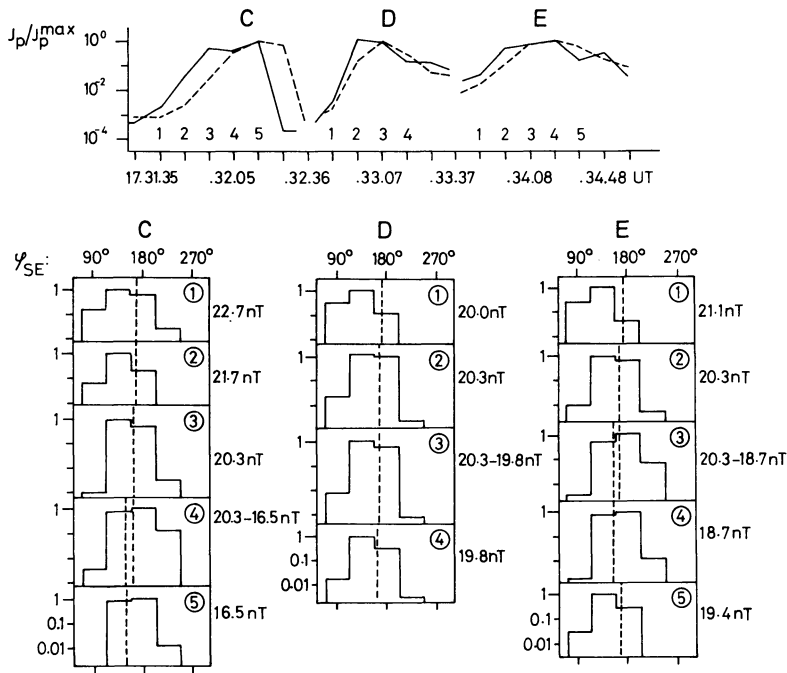


**Fig. 6.** Energy dispersion and pitch-angle distribution of the intense bursts C–E in Fig. 5. *Top*: relative changes in spin-averaged fluxes for 0.29–0.50 MeV (solid line) and 0.5–1.0 MeV (broken line) protons (the fluxes of each channel are normalized to the maximum flux of each burst). *Bottom*: evolution of the flux distribution of 0.29–0.50 MeV protons in the ecliptic plane in the course of each burst. The encircled numbers ①–⑤ indicate the time sector for which the distributions are shown. The fluxes are normalized to the maximum count rate of each time sector. The 15.36-s averages of magnetic field strength are also given for each time sector (two values, if the particle measurement falls between two neighbouring intervals of the magnetic field measurement). The vertical broken line indicates the GSE longitude

#### *HE particle and magnetic field response tailward and earthward of the source region*

The expansion of the most intense substorm on March 3, 1976, started at 17:16 UT. Figure 5 contains the strongest HE proton bursts (for almost all periods of IMP-7 and IMP-8 observations). The ground data published by Sergeev (1981) for this interval show a very rapid and extensive auroral expansion towards 75° CG Lat with clear impulsive substructures. Due to the tailward motion (or jump) of the source region passing over the satellite at 17:36–17:40 UT, the source in this period is first earthward and then tailward of the satellite (see Fig. 2). This may indicate that the source is not so far from the observation site during the 10-min period considered as during other activations of this substorm. Consequently, differences in timing due to different propagation speeds are expected to be smaller. The onsets of the HE particle bursts, therefore, serve well as reference times for the concurrent magnetic variations.

As in Fig. 4, the onsets of the HE particle bursts are indicated in Fig. 5 by broken lines. Once again one can notice the excellent time correlation between these HE particle bursts and those in  $\sigma$ . Again, however, there is no exact intensity correlation between them. The striking difference in the impulse response of  $B_z$  before and after 17:38 UT calls for special attention. Before 17:38 UT (tailward proton flow, source earthward of satellite) the onsets of bursts A–E are followed by a mainly negative  $B_z$  excursion, whereas the  $B_z$  response to the onsets of bursts F–I (source tailward of satellite) is primarily positive. One remarkable additional detail should be noted. The main  $B_z$  excursion is advanced by a short ( $\sim 15$  s) pulse of reverse polarity, and the  $B_y$  component (not shown here, cf. Fig. 5 in Sergeev, 1981) also displays coherent impulsive variations of similar magnitude, being negative before 17:38 and positive after 17:42 UT. It also becomes evident from Fig. 5 that the  $\sigma$  and  $B_x$  responses from both sides of the source region do not differ significantly.

It is of great importance here to ensure the temporal nature of the observed variations (responses). First there is the simultaneity of the onsets of the impulsive rises in both the HE electron and proton fluxes (this is clear for bursts A, D, E, F, G and H). Taking into account the large differences in the gyroradii of both species, this gives the first evidence of the temporal nature of the observed variations. Secondly, we show in the upper part of Fig. 6 the fluxes of 0.3–0.5 MeV and 0.5–1.0 MeV protons (normalized to the maximum flux of each impulse) for the three most intense (superimposed) bursts, C, D and E. The inverse energy dispersion effect is clearly visible. The same effect can also be verified for the bursts F, G and H in Fig. 5. This is further evidence of the temporal nature of the observed variations. Additional evidence comes from the ground-satellite correlation, as will be shown later.

Normalized azimuthal flux distributions of 0.3–0.5 MeV protons are shown in successive frames for each burst in the lower part of Fig. 6. The fluxes are strongly collimated, so that only a portion of the full azimuthal range is displayed. A persistent feature of all three cases of an intense particle burst is that the initial rise in proton counts starts at an  $\sim 45^\circ$  pitch angle. The distribution then shifts towards the field-aligned direction at the time of the burst intensity maximum and turns back to an  $\sim 45^\circ$  pitch angle at the end of the burst. Dawn-to-dusk-directed anisotropy is a common feature of HE protons, and finds its explanation in the N–S gradient of the HE proton number density (Sarris et al., 1976a). This being so, the shift in flux distribution demonstrated here is consistent with the spatial movement of the flux tube containing the highly collimated proton beam, which approaches the satellite and then moves back again. This is also supported by the observations of phases C-4, C-5, E-3 and E-4, when the distributions are obviously shifted towards dawn relative to the local magnetic field direction (broken vertical line). Only at these moments is the satellite embedded in the PS, as evidenced by the lowest values for the magnetic field magnitude ( $B_x$  component),

also presented in Fig. 6, and by the brief spikes in the thermal electron energy density (data kindly provided by E.W. Hones). This “N–S gradient interpretation” thus enables us to see HE field-aligned proton beams whose gyrocentres are contained in the narrow outer boundary part of the PS and which experience local N–S displacements (possible expansion – contraction or flapping motions of the PS) in association with each impulsive activation.

In contrast to the substorm commencing at  $\sim 20$  UT, the HE electrons are found in this case to be highly anisotropic. First, before 17:36 UT, they exhibit a persistent strong tailward anisotropy and then, during the bursts F–H, they occasionally show significant earthward anisotropy (with front-to-back ratio  $> 2$ ). In summary, we can say that the proton and electron data, and also the change in the sign of  $B_z$  at 17:36 UT (Fig. 5), are consistent with a tailward movement of the source region beyond the satellite (for  $T > 17:40$  UT the source is certainly tailward of the satellite).

One of the strongest alpha-particle events in the IMP-J observations is detected in coincidence with the strong proton bursts C–D (cf. Fig. 5), showing that the acceleration mechanism was effective in accelerating charged particles up to a few MeV energy in the same, short (impulsive) process. It is important to note that the proton fluxes in the corresponding energy channel ( $> 2$  MeV) are at least one order of magnitude smaller.

The small time difference ( $\sim 1$  min) between the particle bursts themselves within the first (B–E) and second sequence (F–H) makes it difficult to establish a one-to-one correspondence between them and the individual impulsive activations seen on the ground. In this event, the main information from the ground observations is obtained from an analysis of the Pi-2 signals recorded at auroral and mid-latitudes. The Pi-2 pulsations serve the same purpose here as the earlier Pi1B pulsations shown in Fig. 3. As shown by Sergeev (1981) and supported by an additional data survey, an intense Pi-2 wavetrain starts coherently at widely displaced stations at 17:30:45 UT ( $\pm 5$  s) in coincidence with Pi1Bs, after which an extended, rapid auroral expansion takes place until 17:36 UT. The trains observed at all sites at mid-latitudes display coherent, abrupt phase or amplitude changes, two of which occur at 17:32:30 and 17:34:00 UT, respectively (see Fig. 6 in Sergeev, 1981). A repeated survey including additional data revealed one more coherent change at 17:31:40 UT. These times (triangles at the top of Fig. 5) give an almost exact coincidence of impulsive changes in Pi-2 trains with the onsets of the HE particle bursts B, C, D and E seen at 37  $R_e$ .

The situation after 17:40 UT is not so well suited for a ground-tail comparison, because the various ground observations do not correlate with each other. In particular, the signature of an auroral expansion at very high latitudes (CG Lat  $> 74^\circ$ ) after 17:43–44 UT (see Fig. 2 in Sergeev, 1981) does not correlate with the Pi-2 activity at mid-latitudes, where it is weak and irregular, with the exception of a 2-min pulsation train starting at 17:45:05 UT. Since very high latitude auroral activations are not usually accompanied by clear mid-latitude pulsations in the Pi-2 range (Pytte et al., 1978), and since auroral-zone data alone do not provide sufficient accuracy over the period studied, we cannot support or reject the presence of ground counterparts for bursts F–I in Fig. 5. All that can be said is that the auroral expansion onset and the onset of the mid-lati-

tude Pi-2s seem to be delayed by 1–3 min with respect to the onset of a series of strong HE proton particle bursts. Note that in this case the source region is very much further down the tail than 37  $R_e$ .

## Discussion and conclusions

The observations presented in this paper support the finding of an impulsive energy dissipation process in the substorm expansion phase (Sergeev, 1981; Yahnin et al., 1983). Among the wealth of different variations (temporal and spatial, small- and large-scale), we can apparently distinguish the properties of an “elementary” impulsive process, seen at some distance from the source region. The essential PS features inherent to such an elementary process are summarized below and its physical relevance is discussed.

### *HE particle bursts*

Many impulsive HE particle bursts of short duration were seen at IMP-I or J satellite distances, according to Sarris et al. (1976a, b), Carbary and Krimigis (1979), Lui and Meng (1979), Kirsch et al. (1981); see also the review by Krimigis and Sarris (1979). Bursts of HE electron precipitation (clearly temporal in origin) were often found within the expanding auroral bulge in close association with impulsive Pi activity (Sergeev et al., 1978; Yahnin et al., 1983). Recently, Belian et al. (1984) have reported impulsive structures frequently observed (in more than 75% of all studied cases) in the 0.5-MeV proton injections at geosynchronous orbit. This stresses the generality of the impulsive phenomena with which we are dealing here, and lends further support to the temporal origin of the impulses. In our observations (cf. Figs. 3–5), no significant modulation was found in the individual bursts (at least within the available time resolution of 10 s). The duration of the flux rise is 20–50 s and that of the whole burst  $\sim 1$  min, figures which are in agreement with earlier results (Lui and Meng, 1979). Typically there are intervals of 1–3 min between consecutive bursts. These temporal characteristics agree well with the properties of impulsive structures observed on the ground and at a geosynchronous distance.

Some intense HE proton bursts clearly exhibit the inverse energy dispersion characteristics pointed out earlier for many similar cases by Sarris et al. (1976a) and Kirsch et al. (1981). Strong flux enhancements (up to three orders of magnitude) are seen during some HE particle bursts (e.g. C–E in Figs. 5 and 6), these being practically coherent for electrons and protons having gyroradii of a few hundredths to several  $R_e$ , respectively. Simultaneous impulsive phenomena were recorded on the ground. Taking all these facts together, we may argue that the inverse dispersion effect is due to temporal changes in the efficiency of the acceleration mechanism. Any explanation of the inverse dispersion by spatial effects (velocity filtering), as described by Sarris and Axford (1979) for example, cannot be satisfactory in our case. Firstly it has to be noted that inverse dispersion was observed during a PS boundary which was approaching the satellite, for which Sarris and Axford’s model predicts direct (as opposed to inverse) dispersion (assuming a duskward electric field, as is normal) and, secondly, in the case of Figs. 5 and 6, the source is not very far from the spacecraft (clearly less than 20  $R_e$ ). In this situation an explana-

tion in terms of velocity filtering would require unrealistically large electric fields.

The impulsive acceleration of alpha particles up to 2 MeV in the absence of a similar acceleration of 2-MeV protons was first reported by Kirsch et al. (1981). Similar intense alpha-particle bursts without bursts of protons of corresponding energies were observed on March 3, 1976 in three cases (12:07, 17:18, 22:02 UT) in addition to those presented in Fig. 5, each taking place simultaneously with a strong substorm intensification observed on the ground. The charge dependency of the acceleration process is, therefore, to be regarded as a characteristic of impulsive processes in substorm expansions, which provide particle accelerations up to MeV in tens of seconds.

Dawn-dusk asymmetries in the intensity of HE proton (maximum at dusk) and HE electron fluxes (maximum in the dawn sector of the PS) is known to be a characteristic of HE particle bursts (Krimigis and Sarris, 1979). As shown in paper II, such asymmetries may be a consequence of different longitudinal positions of the satellite (duskwards or dawnwards) relative to the localized active region (auroral bulge). This asymmetry can be very pronounced over a distance less than  $10 R_e$  across the tail (tail width some  $45 R_e$ ) during the initial phase of strong, isolated substorms. Let us compare the ratio of electron to proton fluxes for the studied bursts in relation to the positions of the active region with respect to the satellite as defined from the ground-based data.

In the case of the first substorm presented here (Figs. 3 and 4), the auroral expansion developed mainly to the west of the satellite's meridian before 20:20 UT (paper II). During this period, IMP-J detected the HE electron fluxes well above the level prior to the expansion, which is quite in contrast to the HE proton flux behaviour. Also, the enhancements of the HE fluxes of the bursts are somewhat higher for electrons than for protons during this period. In the case of the second substorm, the expansion region is further west during 17:42–45 UT (bursts F–I) than during 17:30–35 UT (bursts B–E); cf. Fig. 2 of Sergeev (1981). Correspondingly, a pronounced difference is found in the electron/proton content of the bursts between the series C–E and the series F–I in Fig. 5. Thus the acceleration regions seem rather to be localized across the tail and their momentary position apparently defines a demarcation line between the areas of high HE proton and high HE electron flux intensities in the bursts. All these findings are compatible with an acceleration of particles in a localized region in the tail by strong impulsive electric fields.

Due to the limited angular resolution of the CPME experiment and the very large proton gyroradii (in comparison to the thickness of the PS), the ability of this instrument to track movements of HE proton structures within the PS is limited. Nevertheless, we found that in the case where the fluxes are collimated in the direction of the magnetic field lines (e.g. in the cases of Fig. 6) the gyrocentres of protons in HE bursts are contained in a relatively narrow flux tube at the outer boundary of the PS. A similar conclusion was drawn on the basis of the IMP-J measurements for initial phase of substorm expansion (Sergeev, 1983). The presence of a thin layer of energetic protons and alpha particles during both transient and final (recovery) PS expansion was also found by ISEE-1,2 observations made at shorter distances from the earth (Spjeldvik and Fritz, 1981; Möbius et al., 1980; Andrews et al., 1981). This find-

ing can therefore be considered a characteristic feature of the expansion-associated acceleration process, since it is found both earthward and tailward of the source region and since it holds for multiple impulsive bursts (Spjeldvik and Fritz, 1981; Parks et al., 1979 and our results) as well as for the first burst at the expansion onset (Sergeev, 1983).

#### *Propagating magnetic field disturbances and configurational changes of the PS*

The impulsive, discrete, short-lived nature of the expansion process was demonstrated in great detail above. This nature was already suggested by earlier findings (Sergeev and Yahnin, 1979; Sergeev, 1981; Bösinger et al., 1981; Yahnin et al., 1983; Belian et al., 1984). In many previous studies, however, one was looking only for long-lived, large-scale patterns of magnetic field disturbances in the PS presumably caused by reconnection. This pattern is nevertheless strongly contaminated by dynamic small-scale processes, in agreement with the findings of Lui et al. (1977), Coroniti et al. (1980), Kirsch et al. (1981) and Sergeev (1981). Here, therefore, we are looking for an elementary process of explosive dissipation which occurs somewhere in a localized region within the PS.

Around the onset of substorm expansion, the onset of the southward excursion of  $B_z$  in the outer part of the PS at  $37 R_e$  was delayed by about 1 min relative to the arrival of the HE particles. This gives an apparent propagation speed for the magnetic field disturbance relative to the HE particles (see Sergeev, 1983 for other examples) of about  $18 R_e/\text{min}$ , given that the source is at a distance of  $20 R_e$  from the satellite (i.e. at  $15 R_e$  in the nightside PS). This speed is comparable to the speed of sound,  $1,000 \text{ km/s}$  (for  $T_i \sim 6 \text{ keV}$ ), or with the Alfvén speed  $V_A = 0.21 B(\text{nT})/\sqrt{n(\text{cm}^{-3})} R_e/\text{min}$  (for  $B = 20 \text{ nT}$  with  $n = 0.05 \text{ cm}^{-3}$ ) in the PS. We have noted a shortening of this delay for successive activations occurring at progressively higher latitudes in the auroral zone. Finally, there was no delay when the expansion developed at  $\phi = 73^\circ\text{--}75^\circ$  (the source was apparently situated close to the satellite).

The typical patterns of magnetic field variation observed in the outermost part of the PS after an impulsive activation can be produced by a propagating current system of the type shown in the upper part of Fig. 7 (here called the Reconnection Induced Propagating Disturbance – RIPD). The propagation of some kind of current system producing these variations could explain such findings. At least two spacecraft would be needed to verify this, however. This current system must always cause a pronounced southward excursion of the magnetic field within the propagating loop tailward of the source and a short, weak northward excursion ahead of it. A rise in field strength as its front passes by may be expected at the satellite outside or at the outer boundary of the PS. This magnetic field behaviour can be found in the data of Fig. 4 and during the intense bursts A–E displayed in Fig. 5. Earthward of the source the sign of the  $B_z$  variation is reversed, as is in fact observed during bursts F–I shown in Fig. 5. The tail-aligned closure of this current system must exist because of the localization of the source region across the tail.

Such patterns of magnetic field variations are compatible with the recent results of Hones et al. (1982), who studied  $B_y$  variation during substorm onsets. It can be said, however, that the  $B_z$  variations must be more distinct, since



the  $B_x$  and  $B_y$  variations depend in a more complicated way on the position ( $z$ -coordinate) of the satellite with respect to the RIPD. In addition, it can be emphasized that the earthward-propagating part of the RIPD (as discussed by Hill and Reiff, 1980) corresponds well with the three-dimensional system of the substorm current wedge (Akasofu, 1977), which is a well-known phenomenon in the substorm expansion phase. Such a propagating current system (Alfvén wave) must be launched in each act of a localized current disruption which initiates the reconnection process. Similar characteristics of current distribution in the boundary part of the PS were indeed obtained in computer simulation of a three-dimensionally driven reconnection by Sato et al. (1984). It is worthwhile mentioning that the RIPD is qualitatively similar to the meander system introduced by Pellinen and Heikkilä (1984).

As a result of our study, in the lower part of Fig. 7 a schematic and – in view of the complex reality – certainly oversimplified picture is given of what may happen in the tail during successive elementary substorm expansion processes and how this may be embedded into the large-scale “neutral-line-plasmoid” configuration. Several important additions to this scenario should be considered: firstly, the simultaneous presence of several sources, as suggested by the results of Sarris et al. (1976b) and Sergeev and Yahnin (1979), and secondly, an unsystematic change in the source location during successive impulses. The study of auroral arc expansion by Sergeev and Yahnin (1979) and model computations by Forbes and Priest (1983) indeed suggests that new neutral lines may appear at different places in the PS. Note, in Fig. 2, the changes in the directions of arriving HE protons from tailward to earthward and then again to tailward, so that the source may apparently move back and forth.

#### Mechanism of explosive (impulsive) dissipation

The short-lasting impulsive phenomenon of substorm expansion studied here represents the essential (and presumably elementary) part of the whole substorm expansion process, since it provides the significant inputs for auroral expansion, formation of the three-dimensional current system and particle energization and injection. Many of the essential observational signatures of the impulsive process are already known. Most of them have been described in earlier studies (Krimigis and Sarris, 1979; Sergeev, 1981; Kirsch et al., 1981) and are summarized and expanded on in this paper (the first objective). These signatures include:

- the time scale – a few tens of seconds
- acceleration of HE particles in a localized part of the PS up to MeV energies
- indications of acceleration by a strong impulsive electric field (inverse energy dispersion, preferential acceleration of particles with a higher charge, dawn-dusk asymmetry in the acceleration of HE protons and electrons)
- the launching of a three-dimensional current system (like the RIPD) propagating from the source within the  $Y$ -sector of the source location.

Note that the strong impulsive electric field reaching a few tens of mV/m has certainly been detected (Aggson and Heppner, 1977; Pedersen et al., 1978; Cattell et al., 1982). At the present time most of these signatures can be explained by only one mechanism: the non-linear (explosive), collisionless tearing mode (Galeev, 1979). This pro-

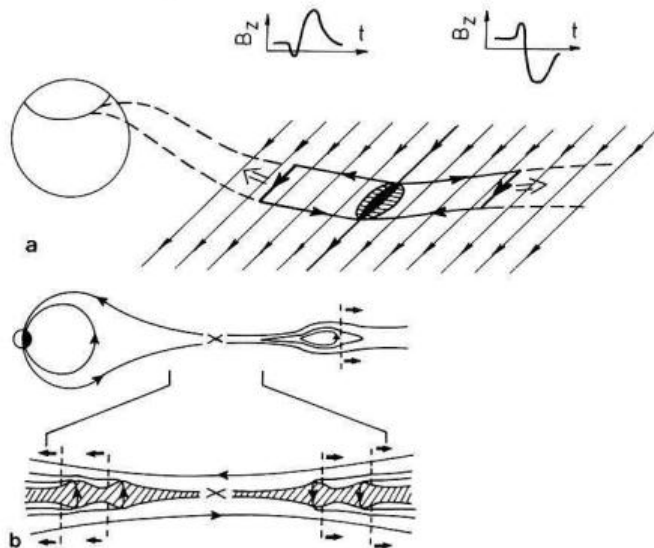


Fig. 7. a Current system (Reconnection Induced Propagating Disturbance – RIPD) launched by each impulse in the explosive expansion process. b Simplified scheme showing the small-scale configurational change in the plasma sheet caused by the inferred impulsive expansion process

vides a consistent explanation for signatures a) – c) and a good description of the spectrum of accelerated ions in the thermal and nonthermal part (Zeleny et al., 1984). This theory has not been completely developed to model the propagation of the magnetic disturbance induced in the PS, but a MHD model describing the latter aspect has recently been developed by Semenov et al. (1983) including, as a particular case, the well-known stationary model of H. Petschek. In spite of inherent simplifications, the model simulates some of the experimental findings of our paper such as a current system of the RIPD type and the swelling of the PS following the propagating RIPD. The model also demonstrates that a transient reconnection is an effective mechanism of energy dissipation.

Both theoretical models are, nevertheless, not yet capable of modelling a real space-time development of the process in a three-dimensional configuration and, in particular, they are not able to produce the repetitive impulsive process. In this respect, the results of a recent numerical MHD modelling within the framework of the line-tied reconnection by Forbes and Priest (1983) deserves special attention. These authors have found very complex behaviour in the system, namely the sporadic growth of a few magnetic islands, corresponding impulsive behaviour of the electric field associated with the growth of each island and a complex movement of active regions back and forth along the tail. Although a collision-dominated process of the tearing mode is not completely realistic in the PS, we find here a time history of the process qualitatively similar to that of the observed expansion process. We conclude that the theoretical attempts yield results basically in agreement with experimental findings, but we must admit that we are still far from achieving a complete insight into the problem.

Our results show how important it is to consider the impulsive, small-scale structures in the PS. At the same time, the large-scale “neutral-line-plasmoid” concept is not excluded by this. On the contrary, many features of our observations are well in tune with the “neutral-line-plas-

moid" concept. Among these features are: the formation of a neutral line in the near-earth region at the substorm onset with preferential tailward anisotropy of HE protons and southward-directed magnetic field deflections at the initial state of substorm expansion (cf. Figs. 2, 4 and 5), the tailward retreat of the main neutral line at the second stage of the expansion with preferential earthward anisotropy of the HE proton and mainly northward-directed magnetic field deflections and, after this, the final PS expansion. One has to be aware that any mode of the reconnection process (impulsive or steady, driven or spontaneous) ends up with the same large-scale configuration and time-averaged properties. In this paper we have looked for, and found, details which can give some insight into the elementary process by which the whole substorm expansion (presumably reconnection) operates in the earth's magnetotail.

*Acknowledgements.* We are indebted to V.S. Semenov and L.M. Zeleny for useful and stimulating discussions. Data on the magnetic field measurements (N. Ness and R. Lepping, principal investigators) and the EPD experiment (D. Williams, principal investigator) onboard the IMP-J satellite were made available through World Data Center A (Rockets and Satellites) by courtesy of J.J. Vette. The data from the LASL thermal plasma experiment were kindly provided by Dr. E.W. Hones. The authors are grateful to A. Yahnin, R. Rachmatulin, E. Barkova, L. Natsvalyan and other colleagues who took part in the collection and preliminary analysis of the ground observations. The work of two of the authors (V.S. and T.B.) is supported by the Finnish-Soviet Committee on Cooperation in Science and Technology, and that of the third author (A.T.Y.L.) by the Atmospheric Sciences section of the National Science Foundation, grant ATM 83-05537 to the Johns Hopkins University.

## References

- Aggson, T.L., Heppner, J.P.: Observations of large transient magnetospheric electric fields. *J. Geophys. Res.* **82**, 5155–5164, 1977
- Akasofu, S.-I.: Physics of magnetospheric substorms. Dordrecht, Holland: D. Reidel 1977
- Andrews, M.K., Keppler, E., Daly, P.W.: Plasma sheet motions inferred from medium-energy ion measurements. *J. Geophys. Res.* **86**, 7543–7556, 1981
- Baker, D.N., Fritz, T.A., Wilken, B., Higbie, P.R., Kaye, S.M., Kivelson, M.G., Moore, T.E., Stüdemann, W., Masley, A.J., Smith, P.H., Vampola, A.L.: Observation and modeling of energetic particles at geosynchronous orbit on July 29, 1977. *J. Geophys. Res.* **87**, 5917–5932, 1982
- Belian, R.D., Baker, D.N., Hones, E.W., Higbie, P.R., Bame, S.J., Asbridge, J.R.: Timing of energetic proton enhancements relative to magnetospheric substorm activity and its implication for substorm theories. *J. Geophys. Res.* **86**, 1415–1421, 1981
- Belian, R.D., Baker, D.N., Hones, E.W., Higbie, P.R.: High-energy proton drift echoes: Multiple peak structure. *J. Geophys. Res.* **89**, 9101–9106, 1984
- Bösinger, T., Alanko, K., Kangas, J., Opgenoorth, H., Baumjohann, W. Correlations between PiB type magnetic micropulsation, auroras, and equivalent current structures during two isolated substorms. *J. Atmos. Terr. Phys.* **53**, 933–945, 1981
- Buck, R.M., West, H.I., D'Arcy, R.G.: Satellite studies of magnetospheric substorms on August 15, 1968. 7. Ogo 5 energetic proton observations – spatial boundaries. *J. Geophys. Res.* **78**, 3103–3118, 1973
- Caan, M.N., Fairfield, D.H., Hones, E.W.: Magnetic fields in flowing magnetotail plasmas and their significance for magnetic reconnection. *J. Geophys. Res.* **84**, 1971–1976, 1979
- Carbary, J.F., Krimigis, S.M.: Energetic particle activity at 5-min and 10-s time resolution in the magnetotail and its relation to auroral activity. *J. Geophys. Res.* **84**, 7123–7137, 1979
- Cattell, C.A., Kim, M., Lin, R.P., Mozer, F.S.: Observations of large electric fields near the plasmasheet boundary by ISEE-1. *Geophys. Res. Lett.* **9**, 539–542, 1982
- Coroniti, F.V., Frank, L.A., Williams, D.J., Lepping, R.P., Scarf, F.L., Krimigis, S.M., Gloeckler, G.: Variability of plasma sheet dynamics. *J. Geophys. Res.* **85**, 2957–2977, 1980
- Forbes, T.G., Priest, E.R.: On reconnection and plasmoids in the geomagnetic tail. *J. Geophys. Res.* **88**, 863–870, 1983
- Galeev, A.A.: Reconnection in the magnetotail. *Space Sci. Rev.* **23**, 411–435, 1979
- Hill, T.W., Reiff, P.H.: Plasma-sheet dynamics and magnetospheric substorms. *Planet. Space Sci.* **28**, 363–374, 1980
- Hones, E.W.: Plasma flow in the magnetotail and its implications for substorm theories. In: Dynamics of the magnetosphere, S.-I. Akasofu, ed.: pp. 545–562. Dordrecht: D. Reidel 1979
- Hones, E.W., Schindler, K.: Magnetotail plasma flow during substorms: a survey with IMP 6 and IMP 8 satellites. *J. Geophys. Res.* **84**, 7155–7169, 1979
- Hones, E.W., Asbridge, J.R., Bame, S.J., Singer, S.: Substorm variations of the magnetotail plasma sheet from  $X \approx -6 R_E$  to  $X \approx -60 R_E$ . *J. Geophys. Res.* **78**, 109–132, 1973
- Hones, E.W., Birn, J., Bame, S.J., Paschmann, G., Russell, C.T.: On the three-dimensional magnetic structure of the plasmoid created in the magnetotail at substorm onset. *Geophys. Res. Lett.* **9**, 203–206, 1982
- Krimigis, S.M., Sarris, E.T.: Energetic particle bursts in the Earth's magnetotail. In: Dynamics of the magnetosphere S.-I. Akasofu, ed.: pp. 599–630. Dordrecht: D. Reidel 1979
- Kirsch, E., Krimigis, S.M., Sarris, E.T., Lepping, R.P.: Detailed study on acceleration and propagation of energetic protons and electrons in the magnetotail during substorm activity. *J. Geophys. Res.* **86**, 6727–6738, 1981
- Lui, A.T.Y., Krimigis, S.M.: Energetic ion beam in the earth's magnetotail lobe. *Geophys. Res. Lett.* **10**, 13–16, 1983
- Lui, A.T.Y., Meng, C.-I.: Relevance of southward magnetic fields in the neutral sheet to anisotropic distribution of energetic electrons and substorm activity. *J. Geophys. Res.* **84**, 5817–5827, 1979
- Lui, A.T.Y., Akasofu, S.-I., Hones, E.W., Bame, S.J., McIlwain, C.E.: Observation of the plasma sheet during a contracted oval substorm in a prolonged quiet period. *J. Geophys. Res.* **81**, 1415–1419, 1976
- Lui, A.T.Y., Meng, C.-I., Akasofu, S.-I.: Search for the magnetic neutral line in the near-earth plasma sheet. 2. Systematic study of IMP 6 magnetic field observations. *J. Geophys. Res.* **82**, 1547–1565, 1977
- Mishin, V.M., Nemtsova, E.I., Saifudinova, T.I., Urbanovich, V.D., Loginov, G.A., Sergeev, V.A., Danilov, A.A., Sobolev, A.V., Solov'ev, S.I., Zaitsev, A.N., Lyubimova, N.P., Shevnina, N.F., Baumjohann, W.: Results of observations during substorms on March 3, 1976. 2. Data of geomagnetic observations. Siberian Institute of Terrestrial Magnetism, Ionosphere and Radio Wave Propagation Preprint Sib-1-82, Irkutsk 1982
- Möbius, E., Ipavich, F.M., Scholer, M., Gloeckler, G., Hovestadt, D., Klecker, B.: Observations of a nonthermal ion layer at the plasma sheet boundary during substorm recovery. *J. Geophys. Res.* **85**, 5143–5148, 1980
- Murayama, T.: Correlated occurrence of energetic electron bursts in the magnetotail and geomagnetic impulsive micropulsation. *Rept. Ionos. Space Res.* **24**, 135–147, 1970
- Nishida, A., Fujii, K.: Thinning of the near-earth (10–15  $R_E$ ) plasma sheet preceding the substorm expansion phase. *Planet. Space Sci.* **24**, 849–853, 1976
- Nishida, A., Hayakawa, H., Hones, E.W.: Observed signatures of reconnection in the magnetotail. *J. Geophys. Res.* **86**, 1422–1436, 1981
- Parks, G.K., Lin, C.S., Anderson, K.A., Lin, R.P., Reme, H.: ISEE 1 and 2 particle observations of outer plasma sheet boundary. *J. Geophys. Res.* **84**, 6471–6476, 1979
- Pedersen, A., Grard, R., Knott, K., Jones, D., Gonfalone, A., Fahlson, U.: Measurements of quasi-static electric fields be-

- tween 3 and 7 earth radii on Geos-1. *Space Sci. Rev.* **22**, 333–346, 1978
- Pellinen, R., Heikkilä, W.J.: Inductive electric fields in the magnetotail and their relation to auroral and substorm phenomena. *Space Sci. Rev.* **37**, 1–61, 1984
- Pudovkin, M.I., Sergeev, V.A. (eds): Results of substorm studies on March 3, 1976. In: *Magnetospheric Res.* (in Russian) **5**, 1984
- Pytte, T., McPherron, R.L., Kivelson, M.G., West, H.I., Hones, E.W.: Multiple-satellite studies of magnetospheric substorms: radial dynamics of the plasma sheet. *J. Geophys. Res.* **81**, 5921–5933, 1976
- Pytte, T., McPherron, R.L., Kivelson, M.G., West, H.I., Hones, E.W.: Multiple-satellite studies of magnetospheric substorms: Plasma sheet recovery and the poleward leap of auroral zone activity. *J. Geophys. Res.* **83**, 5256–5268, 1978
- Roelof, E.C., Keath, E.P., Bostrom, C.O., Williams, D.J.: Fluxes of 50-keV protons and 30-keV electrons at 35  $R_e$ . 1. Velocity anisotropies and plasma flow in the magnetotail. *J. Geophys. Res.* **81**, 2304–2314, 1976
- Sarris, E.T., Axford, W.I.: Energetic protons near the plasma sheet boundary. *Nature* **277**, 460–462, 1979
- Sarris, E.T., Krimigis, S.M., Armstrong, T.P.: Observations of magnetospheric bursts of high-energy protons and electrons at 35  $R_e$  with Imp 7. *J. Geophys. Res.* **81**, 2341–2355, 1976a
- Sarris, E.T., Krimigis, S.M., Iijima, T., Bostrom, C.O., Armstrong, T.P.: Location of the source of magnetospheric energetic particle bursts by multispacecraft observations. *Geophys. Res. Lett.* **3**, 437–440, 1976b
- Sato, T., Walker, R.J., Ashour-Abdalla, M.: Driven magnetic reconnection in three dimensions: Energy conversion and field-aligned current generation. *J. Geophys. Res.* **89**, 9761–9769, 1984
- Semenov, V.S., Heyn, M., Kubyshkin, I.V.: Magnetic field line reconnection in nonstationary case. *Astron J.* (in Russian) **69**, 1138–1147, 1983
- Sergeev, V.A.: On the microstructure of the magnetospheric substorm. *Geomagn. Researches* (in Russian) **21**, 5–15, 1977
- Sergeev, V.A.: High-time resolution correlation between the magnetic field behaviour at 37  $R_e$  distance in the magnetotail plasma sheet and ground phenomena during substorm expansion phase. *J. Geophys. Res.* **49**, 176–185, 1981
- Sergeev, V.A.: Changes in the far plasma sheet at substorm expansion onset. *Geomagn. Aeron.* (in Russian) **23**, 822–828, 1983
- Sergeev, V.A., Yahnin, A.G.: The features of auroral bulge expansion. *Planet. Space Sci.* **27**, 1429–1440, 1979
- Sergeev, V.A., Yahnin, A.G., Raspopov, O.M.: On the spatial-temporal structure of the expansion phase of microsubstorm. In: *Dynamical processes of the auroral magnetosphere* (in Russian), O.M. Raspopov, L.L. Lazutin, eds.: pp. 42–54, Apatity 1978
- Sergeev, V.A., Yahnin, A.G., Gorely, K.I., Danielsen, C., Pellinen, R.I., Samsonov, V.P., Urbanovieh, V.D., Latov, Y.O., Ranta, H., Stauning, P., Armstrong, T.P., Hones, E.W., Krimigis, S.M., Lepping, R.R., Ness, N.F.: Results of observations during substorms on March 3, 1976. 1. Auroral precipitation data and measurements in the magnetotail. Polar Geophysical Institute preprint PGI-81-1, Apatity 1981
- Sergeev, V.A., Pellinen, R.J., Bösinger, T., Baumjohann, W., Stauning, P., Lui, A.T.Y.: Spatial and temporal characteristics of impulsive structure of magnetospheric substorm. *J. Geophys. Res.* **60**, 186–198, 1986
- Spjeldvik, W.N., Fritz, T.A.: Energetic ion and electron observations of the geomagnetic plasma sheet boundary layer: Three-dimensional results from ISEE 1. *J. Geophys. Res.* **86**, 2480–2486, 1981
- Williams, D.J.: Energetic ion beams at the edge of the plasma sheet: ISEE 1 observations plus a simple explanatory model. *J. Geophys. Res.* **66**, 5507–5518, 1981
- Wolcott, J.H., Pongratz, M.B., Hones, E.W., Peterson, R.W.: Correlated observations of two auroral substorms from an aircraft and from a Vela satellite. *J. Geophys. Res.* **81**, 2709–2718, 1976
- Yahnin, A.G., Sergeev, V.A., Pellinen, R.J., Baumjohann, W., Kaila, K.U., Ranta, H., Kangas, J., Raspopov, O.M.: Substorm time sequence and microstructure on 11 November 1976. *J. Geophys. Res.* **53**, 182–197, 1983
- Yahnin, A.G., Sergeev, V.A., Ievenko, I.B., Solovjev, S.I., Rakhmatulin, R.: Characteristics of phenomena accompanied by the local flares of discrete auroras. In: *Magnetospheric Res.* (in Russian) **5**, 93–110, 1984
- Zeleny, L.M., Lipatov, A.S., Lominadze, D.G., Taktakishvili, A.L.: The dynamics of the energetic proton bursts in the course of the magnetic field topology reconstruction in the Earth's magnetotail. *Planet. Space Sci.* **32**, 313–324, 1984

Received August 22, 1984;  
 revised July 23, 1985 and June 2, 1986  
 Accepted July 21, 1986